

Unicentric or Multicentric Castleman disease?

A case report of a pelvic intraperitoneal mass in a middle aged woman

Antonella Smedile^{1*}, Francesca Capuano², Sara Fraticelli², Marco Lucioni², Alfredo La Fianza¹

1. Department of Diagnostic Imaging Institute of Radiology, IRCCS Foundation Policlinic San Matteo, University of Pavia, Pavia, Italy

2. Department of Anatomic Pathology, IRCCS Foundation Policlinic San Matteo, University of Pavia, Pavia, Italy

* **Correspondence:** Antonella Smedile, IRCCS Foundation Policlinic San Matteo, University of Pavia, Pavia, Italy
(✉ antonella.smedile2@gmail.com)

Radiology Case. 2019 Mar; 13(3):28-36 :: DOI: 10.3941/jrcr.v13i3.3387

ABSTRACT

Castleman Disease is a lymphoid disorder characterized by the presence of an enlarged or abnormal lymph node/lymphatic tissue. The disease is classified into unicentric or multicentric variants. The unicentric form is a benign disorder that is usually asymptomatic and consists of a single lymphoid mass that is predominantly located in the mediastinum, but can also rarely develop in the neck or abdomen. The multicentric type involves more than one lymphatic station and is related to the presence of type B symptoms (fevers, night sweats and weight loss), HIV/HHV8 infection and increased serum IL-6 levels. We present the case of an unusual pelvic intraperitoneal manifestation of Castleman Disease in a 52-year-old caucasian woman who showed clinical, radiological, histological and laboratory findings common to both Unicentric and Multicentric Castleman Disease.

CASE REPORT

CASE REPORT

A 52-year-old caucasian woman, with history of ovarian pelvic pain and without any other systemic symptom or disease, underwent a routine transabdominal and transvaginal ultrasonography (US), which reported a solid heterogeneous ovarian lesion with a maximum diameter of 5 x 3 cm, lobulated margins and a peripheral hypervascularity at color-doppler (Fig. 1, Fig. 2).

A contrast-enhanced abdominal computed tomography (CT) examination was performed shortly after at our Institution and revealed a right-pelvis centered 4.7 cm sized intraperitoneal solid mass (113 HU after contrast administration), with regular but lobulated margins and several

intralesional punctate calcifications; an isolated enlarged right obturator lymph node was documented as well (maximum diameter of 26 mm) (Fig. 3, Fig. 4).

Due to shape, location and unknown nature of the described mass, the patient underwent a whole-body ¹⁸F-FDG positron emission tomography (PET) that showed a moderate hypermetabolic activity (SUV_{max} 5) of both the ovarian lesion and of the enlarged ipsilateral obturator lymph node (Fig. 5, Fig. 6).

As a consequence, the patient underwent an explorative laparoscopic surgery at our Institution, in which the intraperitoneal mass was excised.

At histologic examination the mass presented as a lymph node with peculiar features: several B-cell (CD20+, CD79a+) lymphoid follicles were found, with a variable histologic appearance, the majority showing regressively transformed B cell lymphomas-2 (Bcl-2) negative germinal centers, mainly consisting of follicular dendritic cells (CD21+, CD23+), with an expanded mantle region around and a hypervascular interfollicular zone (Fig. 7 a, b, d). The mantle cells formed concentric rings around FDCs (onion skin pattern). Some vascular hyalinized vessels radially penetrated into the germinal center to form the characteristic “lollipop” follicles (Fig. 7 b). The interfollicular area contained increased number of high endothelial venules and small CD3+ T-cell lymphocytes. The immunohistochemical staining for HHV8-related proteins was unremarkable. On the base of such findings, a histopathological diagnosis of hyaline-vascular type Castleman Disease (CD) was suggested. Once the histopathological diagnosis was confirmed, a blood panel performed revealed a mild reduction of WBC (2550/mm³) with neutropenia (1700/mm³) and lymphopenia (500/mm³), a mild increase of light chain K and in K/λ rate (2.1), normal levels of LDH and β2 microglobulin. Immunostaining and urine exam were unremarkable, nonetheless a mild increase in serum level of IL-6 was detected. Serologies for HIV, HCV, HBV and HHV8 were unremarkable.

These finding were unable to fully confirm the supposed diagnosis of Unicentric Castleman Disease; in fact, even if virology was negative for a forementioned viruses and histological finding of hyaline-vascular pattern is commonly linked to this variant of Castleman disease, the presence of two pathological masses and the increase of IL-6 serum levels supported the theory of a Multicentric Castleman Disease (MCD). Two months later another follow-up CT examination was performed, demonstrating no recurrence of the mass (Fig. 8 a), and the persistence of the enlarged right obturator lymph node (Fig. 8 b), though it did not show a hypermetabolic activity at another ¹⁸F-FDG-PET examination (Fig. 9). Moreover the patient did not complain about pelvic pain.

The patient is still in clinical, radiological and laboratory follow-up, with no evidence of recurrent disease.

The presented case report revealed characteristics common to both Unicentric and Multicentric Castleman Disease: the patient did not show typical B symptoms (fevers, night sweats and weight loss), yet with laboratory indices impairment, especially of IL-6 levels. A CT scans demonstrated two pathological pelvic lesions: the largest being a right pelvic mass, yet with histology consistent for Hyaline Vascular-Castleman Disease and negative HHV8 immunostaining, the other an enlarged ipsilateral obturator lymph node.

A short-term post-operative follow up CT performed two months after the surgical removal of the larger mass confirmed the persistence of the enlarged obturator lymph node, but with no pathologic metabolic activity at PET. Moreover IL-6 serum level had got back into the normal range and the patient referred to get healthy. As a consequence, the diagnosis of Unicentric Castleman disease was achieved.

DISCUSSION

Etiology & Demographics:

Castleman Disease (CD), also known as angiofollicular lymph node hyperplasia, was described for the first time in 1956, when Benjamin Castleman reported a series of 13 subjects with localized enlargement of mediastinal hypervascular lymph nodes [1][2][3].

Castleman Disease is a rare benign lymphoid disorder with a heterogeneous clinical presentation and unknown etiology, and is classified into two main different forms. The most frequent Unicentric form, (incidence of 16 cases/million person years [4]) is commonly diagnosed in the third or fourth decade of life and shows a modest female predominance [5], whereas the Multicentric form has an estimated incidence of 5 cases/million person years [4] and typically occurs in older subjects, usually around their sixth decade, with a slightly higher prevalence in males [5]. A third form of Castleman Disease, described as a variant of Multicentric Castleman Disease and linked to HHV8 co-infection, was recently defined, showing a variable incidence and mostly affecting HIV seropositive males [4].

Clinical & Imaging findings:

Castleman Disease can be clinically and radiologically divided into two different forms: the Unicentric form (UCD) which is usually asymptomatic, and the Multicentric form (MCD) which has a higher rate of systemic manifestations and shows increased serum IL-6 levels and a worse prognosis [2][3][5][6][7].

Histologically, there are now four recognized subtypes of CD: the hyaline-vascular type (HV-CD) (76-91% of UCD cases), the plasmacellular variant (PC-CD), HHV-8 associated type (especially in HIV-patients), and the multicentric CD NOS (not otherwise specified) type [5][8][9][7].

UCD is usually asymptomatic at the time of diagnosis and is usually discovered at radiological examinations performed for other reasons. It is more commonly detected in the chest (30%), whereas several cases have been reported in the neck (23%), abdomen (20%), retroperitoneum (17%) and rarely in the axilla (5%), the groin (3%) and the pelvis (2%)[3].

Both MRI and CT are used to evaluate the CD lymphoid masses, but a definitive diagnosis of Castleman Disease is usually based on the histopathological examination [7][10].

The abdominal and pelvic localizations of HV-CD (the presented case and also the most common variant) are commonly characterized at CT imaging by a single, well defined, homogeneous soft-tissue attenuation mass with marked or moderate enhancement after contrast administration. Masses larger than 5 cm in their maximum diameter can additionally show central low attenuation due to central fibrosis or necrosis. Intralesional calcifications occur in 30% of cases [11]. A peripheral rim-like enhancement of the mass, especially evident in the arterial phase, or a local peritoneal thickening around the main mass can also be found [12].

At MRI, pelvic Unicentric Castleman Disease lesions typically appear as hypointense on T1-weighted images and hyperintense on T2-weighted images, but such characteristics are unspecific [7].

Whole-body PET has a role to assess the metabolic status of masses/enlarged lymph nodes suspected for CD. ¹⁸F-FDG-PET allows the recognition of high metabolic uptakes even in non-enlarged lymph nodes, thus playing a role in both staging and monitoring of the disease[8].

Laboratory abnormalities, like anemia and elevation of inflammatory markers, or the presence of type B symptoms (fevers, night sweats and weight loss) are extremely rare in UCD, but can be more frequently observed in histologically proven PC-CD [3], which occurs in only few UCD cases (9-24% of the total) [6].

MCD represent the “dark side” of Castleman disease. HIV infection is an important risk and bad prognosis factor, but all HIV positive patients develop the MCD are co-infected with HHV8. HHV8 can also affect HIV negative patients, and is present in 50% cases of MCD arising in HIV negative patients. The remaining 50% of MCDs have histopathological feature consistent with the PC-CD variant [3].

The majority of MCD patients present with type B symptoms, multiple lymphadenopathies, hepatosplenomegaly and fluid retention within the third space. Laboratory abnormalities, such as the increase of inflammatory markers and more specifically of cytokine levels (IL-6 above all) are common in these patients [3].

At imaging, multiple lymphadenopathies are commonly found in MCD. HV-CD and PC-CD show different CT enhancement patterns, respectively more prominent for HV-CD and less relevant for PC-CD. Such finding, however, is not sufficient to distinguish between the histologic subtypes [13].

Treatment & Prognosis:

Patients with UCD have nearly 100%-5-year survival following *en bloc* surgical resection [7]; patients unsuitable for surgery can undergo radiation therapy [3]. The surgical removal of the lymphoid tissue eliminates the clinical symptoms, if present, and reduces IL-6 serum levels [14].

Due to the risk of lymphomatous conversion of the lymphoid masses and to the possibility of developing a lymphoma in other sites, a post-surgical clinical-radiological surveillance is recommended. The follow-up of these patients should therefore include an annual ¹⁸F-FDG-PET and serum biomarkers (IL-6, CRP, serum free light chains, and quantitative immunoglobulins) [8].

Treatment of MCD is based on corticosteroid, chemotherapy, monoclonal antibodies and radiotherapy and, in certain cases, on combined therapy; MCD, however, is difficult to be treated and completely eradicated [3][7].

Differential Diagnosis:

UCD shows unspecific imaging features. At CT examination UCD can be described as a single, well-defined mass with homogeneous soft-tissue attenuation marked or moderated enhancement in the post-contrast arterial phase and punctate calcifications. At MRI examination, UCD characteristics include T1-hypointensity, T2 hyperintensity and contrast enhancement after gadolinium administration.

The differential diagnosis for abdominal-pelvic UCD include lymphomas, retroperitoneal sarcoma, desmoid tumors [8] and metastatic disease.

Conversely, differential diagnosis of MCD includes lymphomas, infections and immunological diseases like systemic lupus erythematosus (SLE); in HIV seropositive subjects, also persistent generalized lymphadenopathies (PGL) should be taken into account as a mimicker [2].

Whole body PET demonstrates an elevated glucose uptake in both enlarged and in non-enlarged nodes but generally, in CD masses, FDG uptake is less prominent than what is observed in lymphomas [2].

In conclusion, when a single, well-defined, homogeneous soft-tissue attenuation abdominal-pelvic mass or a single enlarged lymph node with marked or moderate enhancement is detected at CT examination, Unicentric Castleman disease should be included in the differential diagnosis and an excisional biopsy should be performed for confirmation.

TEACHING POINT

Unicentric Castleman disease (UCD) should be considered when a single, well defined, homogeneous soft-tissue attenuation contrast-enhancing abdominal mass is detected at CT in an asymptomatic patient. Even though imaging may be suggestive, a histological confirmation is still required for definitive diagnosis and to differentiate it from metastatic disease, lymphoproliferative disorders and other hyper vascularized masses.

REFERENCES

1. Cabot RC, Castleman B, Towne VW. CASE records of the Massachusetts General Hospital Weekly Clinicopathological Exercises: Case 40011. N. Engl. J. Med. 1954. PMID: 13194083
2. Bonekamp D, Horton KM, Hruban RH, Fishman EK. Castleman Disease: The Great Mimic. RadioGraphics, 2011. PMID: 24929266
3. Soumerai JD, Sohani AR, Abramson JS. Diagnosis and management of Castleman disease. Cancer Control, 2014. PMID: 25310208

4. Simpson D. Epidemiology of Castleman Disease. *Hematology/Oncology Clinics of North America*. 2018. PMID: 29157611
5. Talat N, Belgaumkar AP, Schulte KM. Surgery in castlemans disease: A systematic review of 404 published cases. *Annals of Surgery*. 2012. PMID: 22367441
6. Cervantes CE, Correa R. Castleman Disease: A Rare Condition with Endocrine Manifestations. *Cureus*, 2015. PMID: 26719823
7. Guthrie PJ, Thomas JV, Peker D, Turkbey B, Rais-Bahrami S. Perivesical unicentric Castleman disease initially suspected to be metastatic prostate cancer. *Urol Ann*, 2016. PMID: 27141204
8. Madan R., Chen JH, Trotman-Dickenson B, Jacobson F, Hunsaker A. The spectrum of Castleman's disease: Mimics, radiologic pathologic correlation and role of imaging in patient management. *Eur. J. Radiol*. 2012. PMID: 20643523
9. Polizzotto MN, et al. Human and viral interleukin-6 and other cytokines in Kaposi sarcoma herpesvirus-associated multicentric Castleman disease. *Blood*, 2013. PMID: 24174627
10. Hatanaka K, Yoshioka T, Tasaki T, Tanimoto A. The hyaline vascular type of Castleman's disease of the ovary: A case report. *Int. J. Surg. Pathol*. 2014. PMID 24401192
11. Meador TL, McLarney JK. CT features of Castleman disease of the abdomen and pelvis. *AJR. American journal of roentgenology*. 2000. PMID: 10882258
12. Zheng X, Pan K, Cheng J, Dong L, Yang K, Wu E. Localized Castleman disease in retroperitoneum: Newly discovered features by multi-detector helical CT. *Abdom. Imaging*, 2008. PMID: 17619097
13. Kim TJ, Han JK, Kim YH, Kim TK, Choi BI. Castleman disease of the abdomen: Imaging spectrum and clinicopathologic correlations. *J. Comput. Assist. Tomogr*. 2001. PMID: 11242214
14. Yoshizaki K, Murayama S, Ito H, Koga T. The Role of Interleukin-6 in Castleman Disease. *Hematol. Oncol. Clin. North Am*. 2018. PMID: 2788466
15. Raptopoulos V, Gourtsoyiannis N. Peritoneal carcinomatosis. *Eur. Radiol*. 2001. PMID: 11702160
16. Hedgire SS, et al. Extranodal lymphomas of abdomen and pelvis: imaging findings and differential diagnosis. *Abdominal Radiology*. 2017. PMID: 27866240
17. Anthony MP, Khong PL, Zhang J. Spectrum of 18F-FDG PET/CT appearances in peritoneal disease. *Am. J. Roentgenol*. 2009. PMID: 19933627

FIGURES

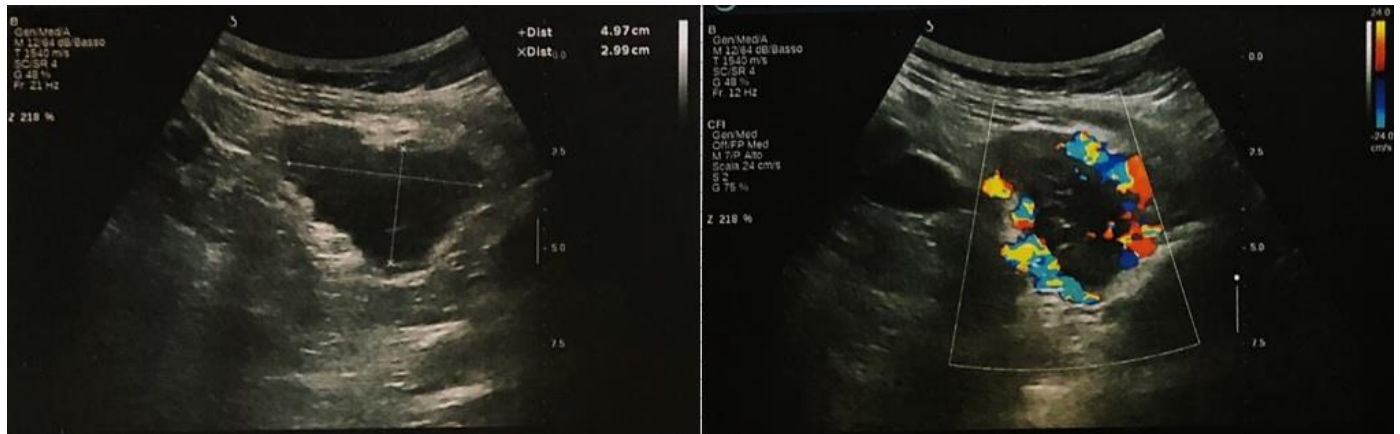


Figure 1: 52-year-old female with Castleman disease.
FINDINGS: Transabdominal ultrasonography revealed an heterogeneous hypoechoic solid lesion, located into the right pelvis. The mass was situated near the right ovary, without a secure cleavage plan. The lesion showed a maximum diameter of 5 x 3 cm, with lobulated margins and with peripheral hypervascularity at color-doppler. Uterine leiomyoma and a small amount of free fluid into the rectouterine pouch were also detected.
TECHNIQUE: Ultrasound, convex probe, 12-21 Hz

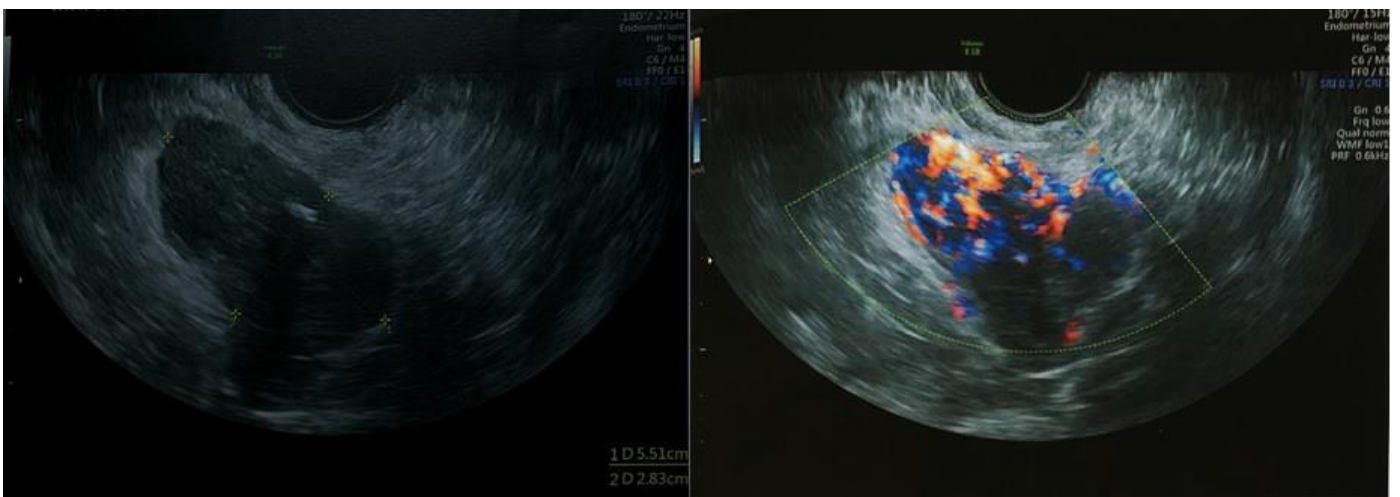


Figure 2: 52-year-old female with Castleman disease.
FINDINGS: Transvaginal ultrasonography confirmed the presence of a heterogeneous hypoechoic solid lesion, located into the right pelvis, close to the right ovary. The lesion showed a maximum diameter of 5 x 3 cm, with lobulated margins and with peripheral hypervascularity at color-doppler.
TECHNIQUE: Ultrasound, transvaginal probe, 15-22 Hz



Figure 3 (left): 52-year-old female with Castleman disease.
FINDINGS: Axial contrast enhanced CT of the pelvis in the parenchymal phase demonstrates a voluminous intra-peritoneal right pelvic solid mass (arrow). It is located behind right rectus abdominis muscle, medially respect right superficial femoral vessels and anterior to the uterus. The maximum diameter on the axial plane is of 4,7 cm. The lesion showed 113 HU of peak after contrast administration, displayed regular but lobulated margins and several calcification spots inside. The intraperitoneal location is recognizable due to the moderate upper-external dislocation of external iliac vascular pedicle. Uterine leiomyoma and a small amount of free fluid into the rectouterine pouch were also detected. Neither lytic bone lesions nor sclerotic bone lesions are detectable.
TECHNIQUE: Axial CT, 156mAs, 100kV, 5,00 mm slice thickness, 80 ml Iodixanol 320 mgI/ml.

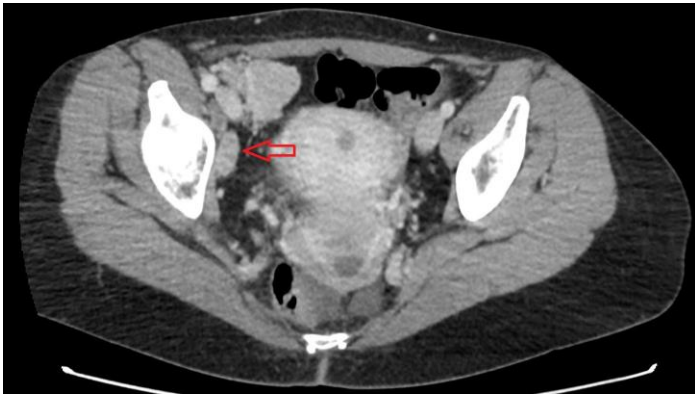


Figure 4 (left): 52-year-old female with Castleman disease. FINDINGS: Axial contrast enhanced CT of the pelvis in the portal phase also shows the presence of an isolated right obturator enlarged lymph node with maximum diameter of 26 mm (arrow). Uterine leiomyoma and a small amount of free fluid into the rectouterine pouch were also detected. Neither lytic bone lesions nor sclerotic bone lesions are detectable. TECHNIQUE: Axial CT, 156mAs, 100kV, 5,00 mm slice thickness, 80 ml Iodixanol 320mgI/ml

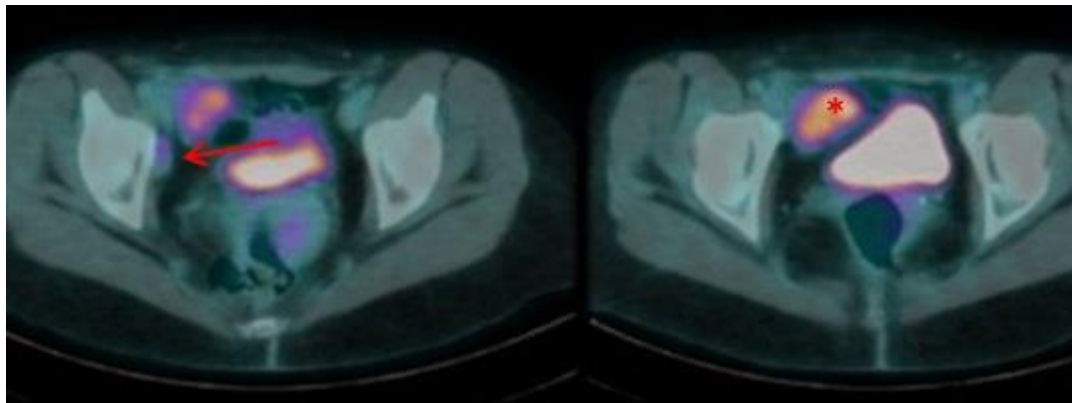


Figure 5: 52-year-old female with Castleman disease. FINDINGS: axial 18F-FDG PET-CT fusion images of the pelvis demonstrate moderate metabolic activity (SUVmax 5) in both the right pelvic mass (asterisk) located near the right ovary, and the right external obturator lymph node (arrow). TECHNIQUE: 18F-FDG-PET, 213 MBq/Kg, 60 min after i.v. injection.



Figure 6 (right): 52-year-old female with Castleman disease. FINDINGS: MIP of the whole-body PET demonstrates two FDG avid areas in the pelvis (SUVmax 5) in both the right pelvic mass (full arrow) and in the right obturator lymph node (empty arrow). TECHNIQUE: 18F-FDG-PET, 213 MBq/Kg, 60 min after i.v. injection.

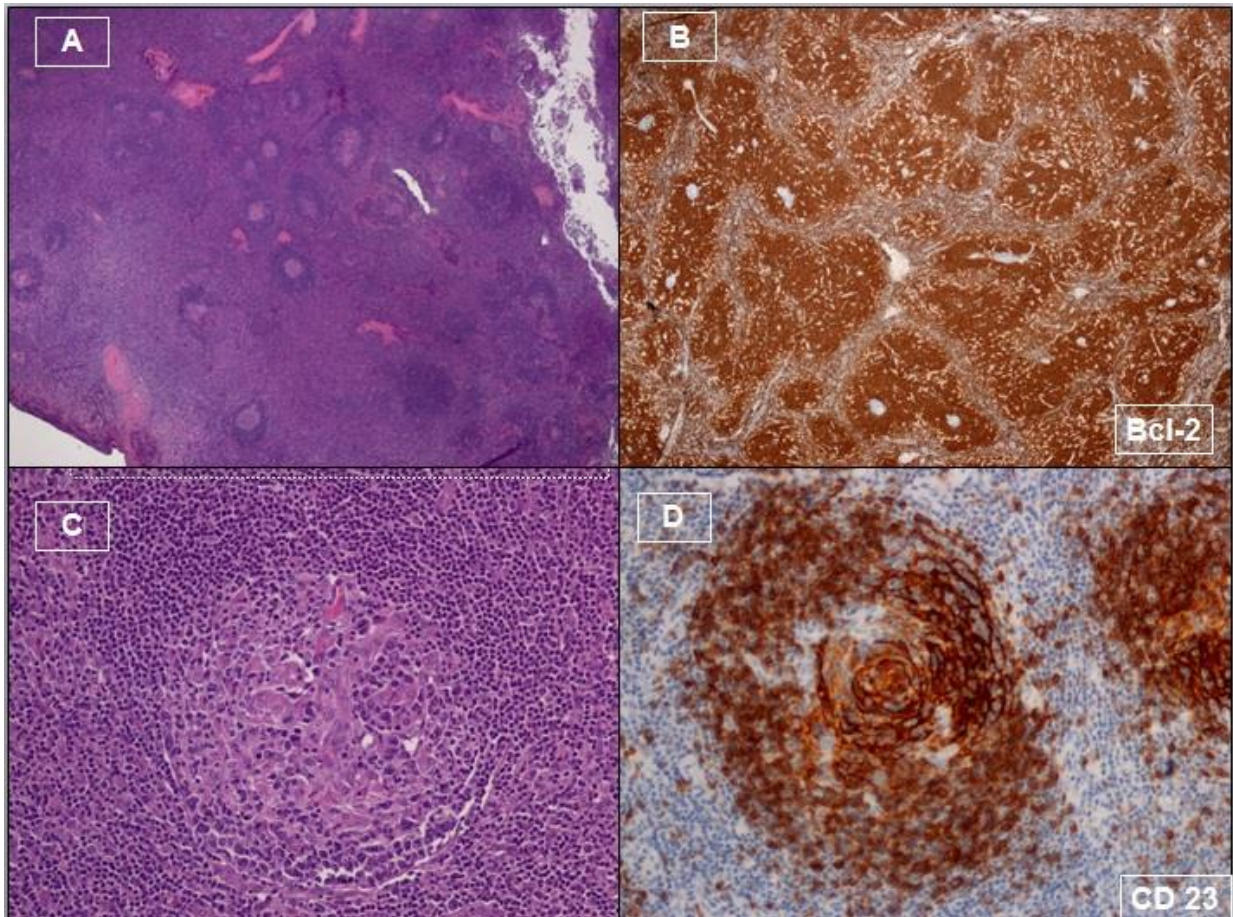


Figure 7: Pathology of 52-year-old female with Castleman disease.

FINDINGS: a) low magnification picture showing several lymphoid follicles, some of them regressively transformed, composed predominantly by FDCs cells with a hyper vascular interfollicular zone. b) (HE 20x) picture showing vascular hyalinized vessels radially penetrated into the germinal center to form the characteristic "lollipop" follicle. c) Immunostaining for Bcl-2 resulting negative on germinal centers, supporting the reactive pattern. d) Immunostaining for CD-23 documenting increased number of FDCs.

TECHNIQUE: a) Hematoxylin- eosin, 2x. b) Hematoxylin- eosin, 20x. c) Immunostaining for Bcl-2 (2x, Envision Flex Peroxidase). d) Immunostaining for Bcl-2 (2x, Envision Flex Peroxidase).

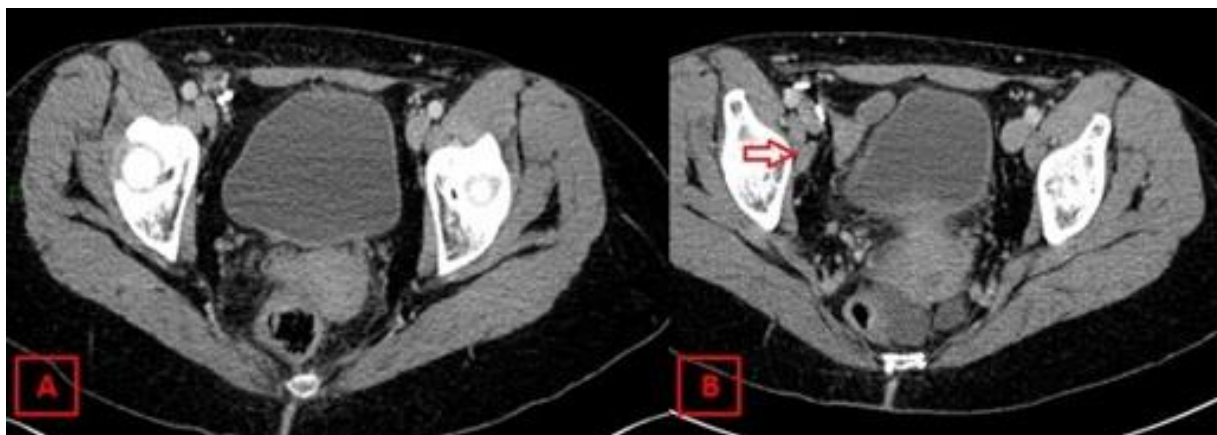


Figure 8: 52-year-old female with Castleman disease.

FINDINGS: Post-surgery axial contrast-enhanced CT of the right pelvis in the parenchymal phase shows no residual mass in right pelvis (A) and the persistence of the enlarged right obturator lymph node (B, empty arrow).

TECHNIQUE: Axial CT, 156mAs, 100kV, 5,00 mm slice thickness, 80 ml Iodixanol 320mgI/ml

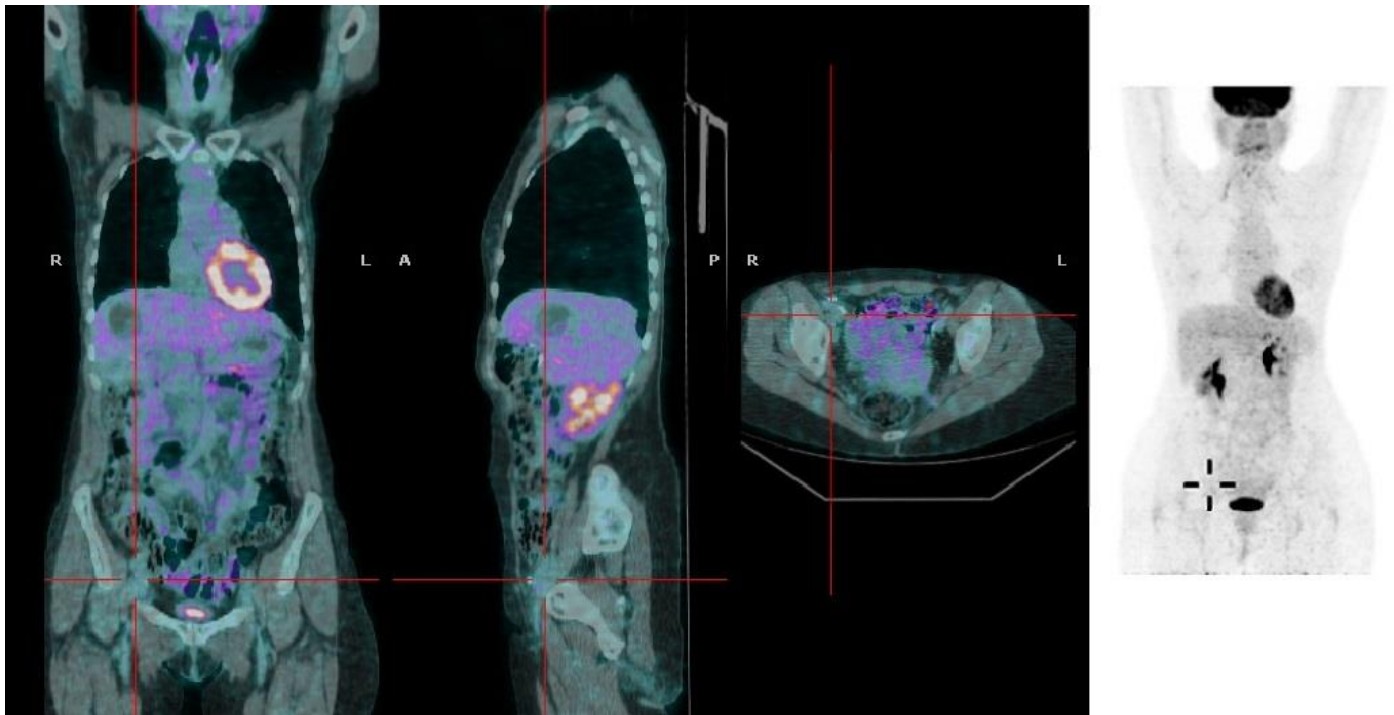


Figure 9: 52-year-old female with Castleman disease.
 FINDINGS: MIP of the whole-body PET and fusion CT-PET images demonstrate no FDG avid areas in the right pelvis, especially in the right obturator lymph node that used to show metabolic activity into pre-operative FDG/PET.
 TECHNIQUE: 18F-FDG-PET, 220 MBq/Kg, 60 min after i.v. injection.

Castleman disease	Unicentric	Multicentric
Etiology	Unknown	HHV8 (especially in HIV-patients)
Incidence	6,500 to 7,700 new cases per year in the US	
Gender	Modest female predominance	Modest male predominance
Age predilection	3rd-4th decade	4th-6th decade
Risk factors	Unknown	HHV8 infection
Treatment	Surgical removal	Monoclonal antibodies and/or radio-chemotherapy
Prognosis	Near 100%-5-year survival	Depends on histological subtype and treatment response
CT features	A single, well defined, homogeneous soft-tissue attenuation mass with marked or moderate enhancement	Diffuse lymph node enlargement

Table 1: Summary table of different types of Castleman disease.

	Unicentric Castleman disease	Metastatic disease	Lymphoproliferative disorder	Malignant mesothelioma
CT	A single, well defined, homogeneous soft-tissue attenuation mass with marked or moderate homogeneous enhancement[11].	Nodules, plaques, sheets of soft tissue, which progress to "omental cake", with contrast enhancement after contrast administration. Calcifications from mucin-producing primary tumors [15]. Usually associated with ascites and lymph node enlargement.	Lobulated masses, with homogeneous contrast enhancement, encasing vessels without displacement ("sandwich sign")[16]. Not significant enhancement or calcifications[11].	Sheets or diffuse thickening of peritoneum, with contrast enhancement after contrast administration [15]. Usually associated with small amount of ascites and lymph node enlargement.
MRI T1	Low signal intensity	Hyperintensity after gadolinium administration	Signal intensity similar to muscle	Hyperintensity after gadolinium administration
MRI T2	High signal intensity	Intermediate signal intensity	Intermediate signal intensity, similar to fat	Intermediate signal intensity
PET	FDG uptake lesser than what observed in lymphomas	Single or multiple enhancing hypermetabolic peritoneal nodules; often associated with ascites with or without FDG avidity[17].	Typically manifest as lymphadenopathy or mimics peritoneal carcinomatosis with mildly diffuse FDG activity and higher uptake in the discrete peritoneal nodules[16].	High FDG avidity seen in solid component[17].

Table 2: Differential diagnoses table for peritoneal pelvic masses.

ABBREVIATIONS

CD = Castleman disease
 HV = Hyaline vascular type
 MCD = Multicentric Castleman disease
 NOS = Non-otherwise specified
 UCD = Unicentric Castleman disease

KEYWORDS

Castleman disease; intraperitoneal mass; lymphoproliferative disorder; unicentric; multicentric

Online access

This publication is online available at:
www.radiologycases.com/index.php/radiologycases/article/view/3387

Peer discussion

Discuss this manuscript in our protected discussion forum at:
www.radiopolis.com/forums/JRCR

Interactivity

This publication is available as an interactive article with scroll, window/level, magnify and more features.
 Available online at www.RadiologyCases.com

Published by EduRad



www.EduRad.org